

HIGH TEMPERATURE MAGNETIC BEHAVIOUR OF IRON-BASED NANOCRYSTALLINE ALLOYS

N. Randrianantoandro, I. Labaye, L. Berger, O. Crisan^a, M. Grafoute, F. Calvayrac
J.-M. Greneche

Laboratoire de Physique de l'Etat Condensé, UMR CNRS 6087, Université du Maine,
72085 Le Mans Cedex 9, France

^aNational Institute for Materials Physics, P.O. Box MG-7, 76900 Bucharest, Romania

After a presentation of structural aspects of iron-based nanocrystalline alloys, the magnetic behaviours of those two-phase magnetic structures are conceptually discussed at high temperatures as a function of the crystalline volumetric fraction, on the basis of the magnetic correlation length compared to the distances between crystalline grains. In addition, some results predicted by an approach based on Monte-Carlo simulation are then briefly presented: they show a qualitative agreement with experimental results.

(Received February 21, 2002; accepted May 15, 2002)

Keywords: Nanocrystalline, Magnetic material, Iron-based alloy

1. Introduction

Over the last decades, the structural [1-4] and magnetic properties [5-7] of nanoscale magnetic materials have been widely investigated because these materials can be applied for magnetic and electromagnetic devices, which require either hard or soft magnetic materials. Soft magnetic applications include inductive devices, transformers while hard magnetic systems are of great interest for permanent magnets and magnetic storage media. It is also important to emphasize the emergence of spring exchange magnets which result from both hard and soft magnetic grains. Their total magnetic properties which do combine both the large coercivities and the large inductions of hard and soft magnetic grains, respectively, are also dependent on the degree of magnetic coupling between the different magnetic phases. The magnetic properties of nanostructured magnets which can be described as nanoscale heterogeneous systems are also dependent on the magnetic nature of the matrix and on the magnetic coupling between the different grains, which is now governed by the magnetic correlation lengths. Indeed, the change from microcrystalline to nanocrystalline scale systems implies to revise some basic concepts to understand their magnetic behaviours.

In microcrystalline magnetic systems, the magnetic energy results from the sum of the field Zeeman energy originated from the exchange coupling, the demagnetization energy, the wall energy due to the presence of both magnetic domains and magnetic walls, and the magnetic anisotropy energy due to magnetocrystalline, shape and stress contributions. It is important to remember that the magnetic anisotropy represents an energy barrier to the magnetization switching. In soft magnetic materials, both the minimum of hysteretic losses and the maximum of permeability are due to small magnetic anisotropy. Low magnetocrystalline anisotropy is thus observed in cubic phases while stress anisotropy is reduced in nearly zero magnetostrictive alloys and shape anisotropy related to demagnetizing effects vanishes with large magnetic grains. Let us note that the lack of crystalline lattice in amorphous alloys favours low magnetic anisotropies. On the contrary, important magnetic anisotropies are required in hard magnetic systems, as induced by anisotropic crystalline structures and large spin-orbit interactions. Finally, the presence of structural defects and impurities, so called pinning sites, and their concentration are the key points for the occurrence of domain walls in multi-domain magnetic materials. The understanding of the nucleation, the propagation and the annihilation of domain walls remains a relevant stage in developing soft magnetic materials. It is thus clearly established that the magnetic performances of soft magnetic materials can be improved after

controlling their microstructures and optimizing the processing conditions, while two-phase microstructures with pinning phases are necessary to enhance magnetic properties in the case of hard magnetic materials. One important characteristic is the magnetic exchange correlation length which has to be compared to the grain size and the distance between grains (noted as Δ), as it is schematized in Fig. 1.

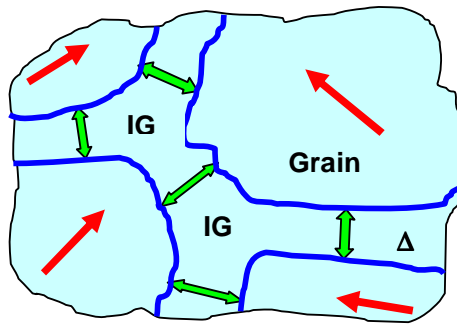


Fig. 1. Schematic representation of a two-phase magnetic system where the magnetic correlation length has to be compared to the intergrain (IG) distance Δ .

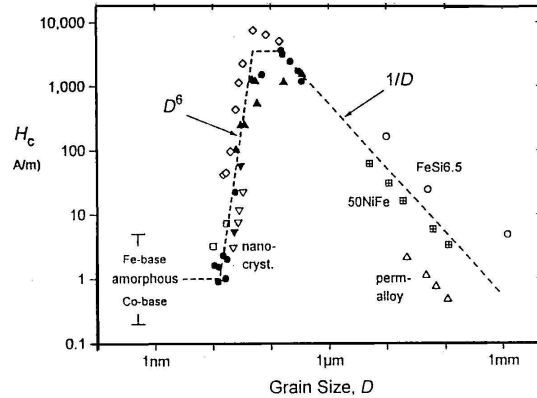


Fig. 2. Coercive field versus grain size where several data are reported and agree with two main behaviours: $1/D$ and D^6 where D is the diameter of the crystalline grain (see text). (after [14]).

Nanocrystalline and nanostructured magnetic systems consist of grains, whose diameter is generally ranging from ~ 1 up to 50 nm. It is thus obvious to understand that the fundamental aspects previously described have to be revised. The different contributions to magnetic anisotropy in nanocrystalline systems strongly differ from those in microcrystalline systems. In addition, the concept of domain walls disappears because the nanocrystalline grains behave as single magnetic domain. However, the magneto-crystalline anisotropy of an assembly of nanocrystalline grains randomly distributed can be modelled by means of the random anisotropy model. This approach initially developed by Alben et al [8] to describe the soft magnetic properties of amorphous ferromagnets, was recently extended by Herzer et al [9] to explain the soft magnetic properties of nanocrystalline alloys. The model predicts thus the strong variation of both the effective anisotropy and the coercive field with the sixth power of the grain size, that is supported by experimental observations as it is shown in Fig. 2.

But in the case of nanoparticles, the thermal energy can be sufficient to reverse the magnetization direction as a consequence of the superparamagnetic relaxation phenomena [10]. Indeed, in the case of fine and ultrafine magnetic particles, the switching of the magnetization over rotational energy barrier, that is provided by magnetic anisotropy, induces a reduction of coercive field and fluctuations. The switching frequency is larger for smaller particle size, smaller anisotropy energy density and at higher temperatures, but decreases in presence of increasing interparticle interactions, i.e. when the distance between particle decreases.

Consequently, a relevant parameter is the degree of dispersion of fine and ultrafine magnetic grains and the magnetic nature of the matrix or of the intergranular phase. The magnetic coupling between grains has to be thus compared to the magnetic correlation length, favouring or disfavouring the interactions between grains. This magnetic correlation length strongly depends on the chemical nature of the materials. Indeed, in the case of insulating systems as fluorides, oxides, the superexchange mechanism based on the overlap of molecular orbitals is large for nearest neighbours and medium for second nearest neighbours (so called supersuperexchange) but can be neglected beyond the third nearest neighbours. On the contrary, the magnetic interactions in metallics are governed by the itinerant electron mechanism (RKKY interaction) Those mechanisms suggest magnetic correlation lengths of approximately 1 nm and 10 nm, respectively.

One can consider that the magnetic domains are extended over many nanocrystalline grains since they are ferromagnetically ordered due to the short-range magnetic exchange interactions at low temperature, i.e. below the Curie temperatures. When the temperature increases, the ferromagnetic-paramagnetic phase transition of one phase causes thus an interruption of the exchange interactions between the two phases which now are competing with magnetic anisotropies. At sufficiently high temperature, the thermal energy might become important, according to the magnetic nanostructure characteristics.

2. Nanocrystalline alloys

Since the pioneering nanocrystalline system discovered by Yoshizawa et al in 1988 [11], the so-called FINEMET (nominal composition $\text{Fe}_{73.5}\text{Cu}_1\text{Nb}_3\text{B}_9\text{Si}_{13.5}$), NANOPERM type alloys (FeMB alloys with $M = \text{Zr}, \text{Hf}, \text{Nb}$) were then prepared by Suzuki et al in 1991 [12] and HITPERM-type alloys ((Fe,Co)-M-B-Cu with $M = \text{Zr}, \text{Hf}, \text{Nb}$) were recently proposed in 1998 by Willard et al [13]. The nanocrystalline alloys result from a subsequent annealing of the amorphous precursors, allowing a controlled volumetric fraction of crystalline grains to be dispersed. The nanocrystalline alloys consist thus of ultrafine crystalline grains embedded within a residual amorphous phase. The nanocrystalline state is due to the two different stages of crystallization: the first stage favours the nanocrystallization while the complete crystallization of the amorphous remaining phase into crystalline grains is achieved at the second stage. The different sequences associated to the transformation from the amorphous to the crystalline state in the case of FINEMET alloys are illustrated in Fig. 3 the FeSi crystalline precipitates exhibit either bcc or DO₃ structures.

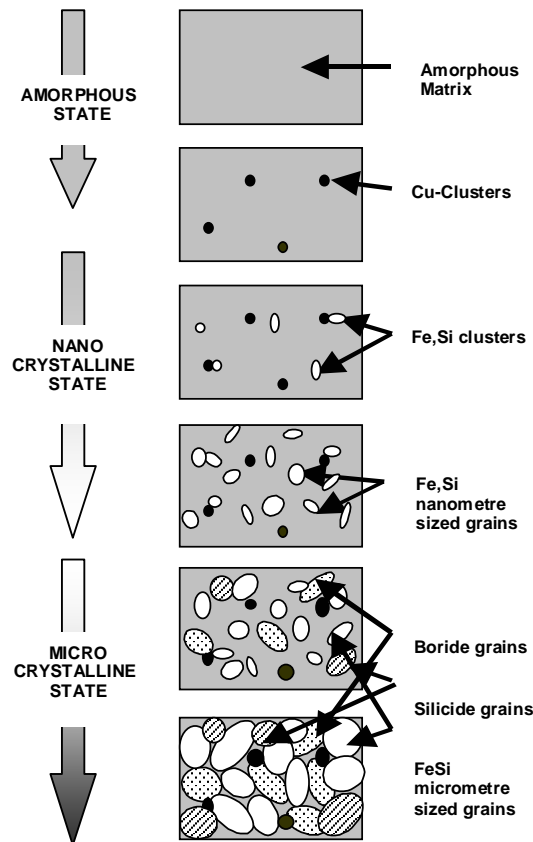


Fig. 3. Schematic representation of the transformation from the amorphous state into the nanocrystalline state and then the complete crystalline state.

This scenario is rather similar to those observed on other kinds of nanocrystalline alloys, except for the crystalline nature nanograins: bcc Fe and bcc FeCo for NANOPERM and HITPERM nanocrystalline alloys, respectively. Some important features have to be emphasized: the size of grains remains weakly independent on the annealing time and the annealing temperature, when it is comprised between the two stages of crystallization. Cu atoms first nucleate into clusters favouring homogeneous nanocrystallization process while M atoms are preferentially located at the periphery of crystalline grains, leading to a barrier-like to the atomic diffusion, preventing thus the growth of the grains (see those reviews and references therein [14, 15]).

It is clear that the resulting magnetic properties of these nanocrystalline alloys are strongly dependent on the temperature and on the volumetric crystalline fraction. It is possible to distinguish *a priori* three magnetic regimes, considering the Curie temperatures of the crystalline grains T_c^{cryst} and of the amorphous matrix T_c^{am} , with $T_c^{\text{cryst}} > T_c^{\text{am}}$. At temperatures higher than T_c^{cryst} , both crystalline grains and amorphous matrix are paramagnetic while below T_c^{am} , both are magnetically ordered and thus strongly coupled through short-range magnetic interactions.

In the intermediate temperature range, $T_c^{\text{am}} < T < T_c^{\text{cryst}}$, the system consists of an assembly of ferromagnetic grains embedded in a paramagnetic amorphous remainder. When the density of grains is low, typically < 20 at. %, the mean distance between grains which is larger than the magnetic correlation length prevents a strong coupling between grains. The ferromagnetic grains can be thus described as an assembly of non-interacting single domain particles embedded in a paramagnetic matrix. Consequently, the thermal energy overcomes the other magnetic energy contributions, giving rise to the presence of magnetization fluctuations. Indeed, the appearance of superparamagnetic fluctuations was clearly evidenced at higher temperature by static magnetic measurements and by ^{57}Fe Mössbauer spectrometry [16, 17]. The thermal energy destabilizes the magnetic state, originating a decrease of coercive field according to the following relationship above the Curie temperature of the amorphous matrix, as predicted by Pfeiffer, $H_c(T) = H_c(0) [1 - T/T_B]^{0.77}$, where $H_c(0)$ is the coercive field at 0K and T_B is the superparamagnetic blocking temperature [18]. Such a situation is illustrated in Fig. 4a. When the density of grains is progressively increasing, one can distinguish two different kinds of grains. There are first magnetically isolated grains, the density of which is decreasing. Then, one observes grains, for which the distance between grains becomes smaller than the magnetic correlation length. Consequently, the decreasing number of uncoupled grains in detriment of an increasing number of coupled grains favours thus a progressive decrease of thermal fluctuation effects at high temperature and a progressive increase of the medium range exchange magnetic interactions (see Fig.s 4b and 4c). But it is difficult to quantify the number of interacting and non-interacting grains, because of the distribution of size, morphology and dispersion within the matrix [19].

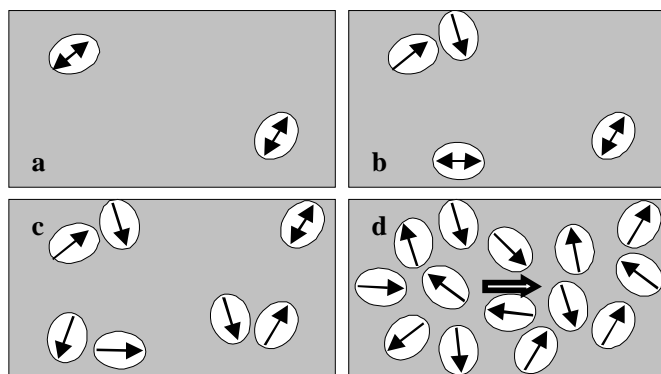


Fig. 4. Schematic representation of magnetic behaviours as a function of the volumetric crystalline fraction. Single array represents blocked magnetization (static regime) while double array symbolizes the presence of magnetization fluctuations in single domain grains, i. e. the superparamagnetic behaviour.

With higher annealing temperatures, the volumetric crystalline fraction tends to be maximum at about 60 - 65 at. % before the transformation from the nanocrystalline state into the microcrystalline state. In such a situation, all the crystalline grains are magnetically coupled because the distance between each grain is smaller than the typical magnetic correlation length, preventing

thus the occurrence of superparamagnetic effects. In other words, both the anisotropy energy contributions and the short range magnetic interactions prevail strongly the thermal energy which is now close to zero. Such phenomena are well supported by static magnetic measurements and Mössbauer spectrometry. In addition, this latter technique revealed that the remaining intergranular phase does not exhibit any pure paramagnetic state, even at temperatures far above the Curie temperature: magnetic interactions between grains originate some penetrating fields which polarize the magnetic moments located in the intergranular phase [20-23]. It is schematically represented in Fig. 4d.

3. Numeric approach of two-phase magnetic system

The magnetic behaviour of these two-phase magnetic nanostructures can be modelled using different approaches: micromagnetism [24, 25], molecular field calculations [26], and effective field theory [27]. We have considered the atomic Monte-Carlo simulations using a classical Metropolis algorithm, because they can provide a modelling of the magnetic configurations in the different zones of the materials, as a function of temperature. In addition, macroscopic thermodynamic functions, such as magnetization, specific heat and magnetic susceptibility for our system can be derived as a function of the temperature.

The sample is represented by a simple cubic lattice containing up to 20^3 Heisenberg type spins, each spin has thus 6 nearest neighbours. Two parts are distinguished: a sphere of radius R (in units of the interatomic structure) to describe the crystalline grain with A spins and the external part which represents the matrix with B spins. Each part is characterized by its own exchange integral interaction (chosen J_{AA} and $J_{BB} > 0$) giving rise to two different Curie temperatures and a third zone corresponding to the interface between the grain and the matrix characterized by both exchange coupling ($J_{AB} > 0$) and interface anisotropy. The computing aspects which are detailed elsewhere, were performed using a home-made parallel computer (Beowulf class) composed of 70 processors (see website: <http://weblotus.uni-llemans.fr/w3lotus>) [28, 29].

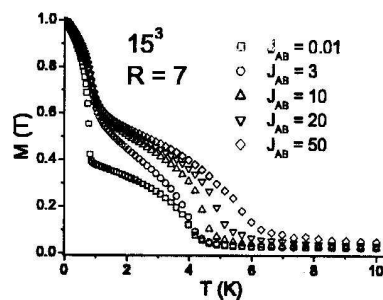


Fig. 5. Temperature dependence of the total normalized magnetization of the system for a nanograin radius of $R = 7$ and for matrix - nanograin exchange coupling J_{AB} ranging from 0.01 to 50.

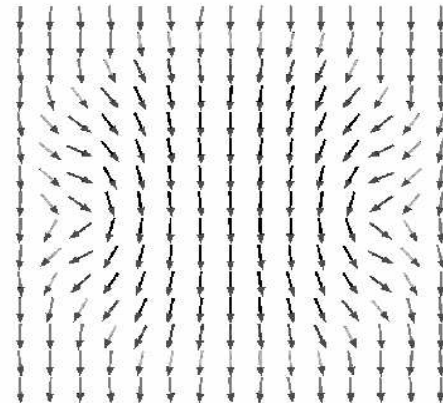


Fig. 6. Example of spin configuration of the middle plane of the cubic lattice (from [23]).

Those calculations allow to model the total magnetic behaviour of the whole system and for the first time to model independently the magnetic behaviours of both the ferromagnetic grain and the ferromagnetic matrix as a function of temperature and as a function of the internal and mutual exchange couplings and of the interface anisotropy. Fig. 5 shows clearly a nearby non-interacting two-phase system ($J_{AB} = 0.01$) with the occurrence of two Curie temperatures; when the interphase coupling (J_{AB}) increases, the evolution of the total magnetization which is qualitatively consistent with

experimental data allows to evidence an increasing spin polarization - depolarization mechanism which induces magnetic correlation between spins. Detailed results are published elsewhere [29]. In addition, 3D magnetic configurations can be proposed from such calculations: an example is illustrated in Fig. 6. A non collinear structure at the interface is clearly evidenced when the interface anisotropy contribution is considered, that is in agreement with a spin-glass-like structure experimentally observed [30].

Acknowledgements

The authors thank to Prof A. Slawska-Waniewska (Warsaw), Dr I. Skorvanek (Kosice), Prof M. Miglierini (Bratislava), Prof J.M.D. Coey (Dublin), and Dr J. Borrego (Sevilla) for fruitful discussions during recent years. The financial support of Region Pays de Loire for the Post-doc position of O.C. at LPEC is gratefully acknowledged.

References

- [1] H. Gleiter, *Prog. Mater. Sci.* **33**, 223 (1989).
- [2] H. Gleiter, *Acta Mater.* **48**, 1 (2000).
- [3] *Nanophase Materials: Synthesis, Properties, and Applications*, Eds. G. C Hadjipanayis and R. W. Siegel, Kluwer Academic Publisher, Dordrecht, p. 515, 1994.
- [4] C. Suryanarayana, C.C. Koch, *Hyper. Inter.* **130**, 5 (2000).
- [5] M. E. Henry, D. E. Laughlin, *Acta Mater.* **48**, 223 (2000).
- [6] A. Hernando, J. M. Gonzales, *Hyper. Inter.* **130**, 221 (2000).
- [7] H. K. Lachowicz, *J. Tech. Phys.* **42**, 127 (2001).
- [8] R. Alben, J. J. Becker, M. C. Chi, *J. Appl. Phys.* **49**, 1653 (1978).
- [9] G. Herzer, *Phys. Scr.* **T49**, 307 (1993).
- [10] J. L. Dormann, D. Fiorani, E. Tronc, *Advances in Chemical Physics Vol. XCVIII*, Eds. I. Prigogine and Stuart A. Rice, John Wiley & Sons Inc., p. 283, 1997.
- [11] Y. Yoshizawa, S. Oguma, K. Yamauchi, *J. Appl. Phys.* **64**, 6044 (1988).
- [12] K. Suzuki, N. Kataoka, A. Inoue, A. Makino, T. Masumoto, *Mat. Trans., JIM* **31**, 743 (1990).
- [13] M. A. Willard, D. E. Laughlin, M. E. McHenry, D. Thoma, K. Sickafus, J. O. Cross, V. G. Harris, *J. Appl. Phys.* **84**, 6773 (1998).
- [14] G. Herzer, *Handbook of Magnetic Materials*, Vol 10, Ed. K. H. J. Buschow, Elsevier Science, Amsterdam, Holland, p. 415, 1997.
- [15] T. Kemény, D. Kaptas, L. F. Kiss, J. Balogh, I. Vincze, S. Szabo, D. L. Beke, *Hyper. Inter.* **130**, 181 (2000).
- [16] A. Slawska-Waniewska, P. Novicki, H. Lachowicz, P. Gorria, J. M. Barandiaran, A. Hernando, *Phys. Rev. B* **50**, 6465 (1994).
- [17] N. Randrianantoandro, A. Slawska-Waniewska and J.M. Grenèche, *Phys. Rev. B* **56**, 10797 (1997).
- [18] H. Pfeiffer, *Phys. Stat. Sol. (a)* **118**, 295 (1990).
- [19] J. M. Grenèche, M. Miglierini, A. Slawska-Waniewska, *Hyper. Inter.* **126**, 27 (2000).
- [20] A. Hernando, T. Kulik, *Phys. Rev. B* **49**, 7064 (1994).
- [21] I. Suzuki, J. M. Cadogan, *Phys. Rev. B* **58**, 2730 (1998).
- [22] J. S. Garitaonandia, D. S. Schmool, J. M. Barandiaran, *Phys. Rev. B* **58**, 12147 (1998).
- [23] I. Škorvánek, J. Kovás, J. M. Grenèche, *J. Phys. Condens. Matter* **12**, 9085 (2000)
- [24] H. Kronmüller, R. Fischer, R. Hertel, T. Leineweber, *J. Magn. Magn. Mater.* **175**, 177 (1997).
- [25] H. Kronmüller, R. Fischer, M. Bachmann, T. Leineweber, *J. Magn. Magn. Mater.* **203**, 12 (1999).
- [26] D. Givord et al., to be submitted.
- [27] T. Kaneyoshi, *J. Phys. Condens. Matter*, **3**, 4497 (1991).
- [28] O. Crisan, Y. Labaye, L. Berger, J. M. D. Coey, J. M. Grenèche, *J. Appl. Phys.* (2002) in press.
- [29] O. Crisan, Y. Labaye, L. Berger, J. M. D. Coey, J. M. Grenèche, to be submitted.
- [30] A. Slawska-Waniewska, J. M. Grenèche, *Phys. Rev. B* **56**, R8491 (1997).